Proteomic landscapes of inherited platelet disorders with different etiologies

Kreft, I.C.; Huisman, E.J.; Cnossen, M.H.; Alphen, F.P.J. van; Zwaan, C. van der; Leeuwen, K. van; ... ; Hoogendijk, A.J.

Received: 2 September 2022 | Revised: 4 November 2022 | Accepted: 16 November 2022

https://doi.org/10.1016/j.jtha.2022.11.021

ORIGINAL ARTICLE

Proteomic landscapes of inherited platelet disorders with different etiologies

Iris C. Kreft[1] | Elise J. Huisman[2,3] | Marjon H. Cnossen[2] | Floris P. J. van Alphen[1] | Carmen van der Zwaan[1] | Karin van Leeuwen[1] | Rosalina van Spaendonk[4,5] | Leendert Porcelijn[6] | Caroline S. B. Veen[7] | Maartje van den Biggelaar[1,8] | Masja de Haas[9,10] | Alexander B. Meijer[1,8] | Arie J. Hoogendijk[1]

[1]Department of Molecular Hematology, Sanquin Research, Amsterdam, The Netherlands

[2]Department of Pediatric Hematology, Erasmus MC Sophia Children's Hospital, University Medical Center Rotterdam, The Netherlands

[3]Unit of Transfusion Medicine, Sanquin Blood Supply, Amsterdam, The Netherlands

[4]Department of Immunohematology Diagnostic, Sanquin Diagnostic Services, Amsterdam, The Netherlands

[5]Department of Human Genetics, Amsterdam University Medical Center, Amsterdam, The Netherlands

[6]Department of Immunohematology and Blood Transfusion, Leiden University Medical Center, Leiden, The Netherlands

[7]Department of Hematology, Erasmus MC, University Medical Center Rotterdam, The Netherlands

[8]Utrecht Institute for Pharmaceutical Sciences, Utrecht University, Utrecht, The Netherlands

[9]Department of Hematology, Leiden University Medical Center, Leiden, The Netherlands

[10]Center for Clinical Transfusion Research, Sanquin Research, Amsterdam and Landsteiner Laboratory, Academic Medical Centre, University of Amsterdam, Amsterdam, The Netherlands

Abstract

Background: Inherited platelet disorders (IPDs) are a heterogeneous group of rare diseases that are caused by the defects in early megakaryopoiesis, proplatelet formation, and/or mature platelet function. Although genomic sequencing is increasingly used to identify genetic variants underlying IPD, this technique does not disclose resulting molecular changes that impact platelet function. Proteins are the functional units that shape platelet function; however, insights into how variants that cause IPDs impact platelet proteomes are limited.

Objectives: The objective of this study was to profile the platelet proteomics signatures of IPDs.

Methods: We performed unbiased label-free quantitative mass spectrometry (MS)–based proteome profiling on platelets of 34 patients with IPDs with variants in 13 ISTH TIER1 genes that affect different stages of platelet development.

Results: In line with the phenotypical heterogeneity between IPDs, proteomes were diverse between IPDs. We observed extensive proteomic alterations in patients with a *GFI1B* variant and for genetic variants in genes encoding proteins that impact cytoskeletal processes (*MYH9*, *TUBB1*, and *WAS*). Using the diversity between IPDs, we clustered protein dynamics, revealing disrupted protein-protein complexes. This analysis furthermore grouped proteins with similar cellular function and location, classifying mitochondrial protein constituents and identifying both known and putative novel alpha granule associated proteins.

Conclusions: With this study, we demonstrate a MS–based proteomics perspective to IPDs. By integrating the effects of IPDs that impact different aspects of platelet function, we dissected the biological contexts of protein alterations to gain further insights into the biology of platelet (dys)function.

Manuscript handled by: Keith Neeves

Final decision: Keith Neeves, 17 November 2022

Iris C. Kreft and Elise J. Huisman are co-first authors to this study.

Correspondence Arie J. Hoogendijk, Department of Molecular Hematology, Sanquin Research, Plesmanlaan 125, 1066 CX, Amsterdam, The Netherlands.
Email: a.hoogendijk@sanquin.nl

KEYWORDS
blood platelets, inherited blood coagulation disorders, mass spectrometry, multiprotein complexes, proteomics

1 | INTRODUCTION

Platelets are anucleated cell fragments that are released by megakaryocytes into the circulation and play a crucial role in primary hemostasis. Activation of platelets induces granule release, shape change, and aggregation, ultimately resulting in the formation of a platelet plug that restores vascular integrity and limits blood loss [1]. Inherited platelet disorders (IPDs) are a heterogeneous group of rare bleeding disorders with varying clinical expression and an increased bleeding tendency as a common denominator [2]. Gene variants causing IPDs may disrupt hematopoietic stem cell commitment to megakaryocyte lineage, megakaryocyte proliferation and terminal differentiation, proplatelet formation, or platelet shedding. Therefore, IPDs may exhibit impairments in the production of sufficient platelet numbers (ie, thrombocytopenia) and in the function of circulating platelets (ie, thrombocytopathy) [3]. Diagnosis of IPDs is increasingly performed by using high-throughput DNA sequencing [4–7]. This development is supported by the establishment of curated disease-causing (ISTH TIER1) genes and the gold variant resources for inherited bleeding, platelet, or thrombotic disorders [6]. However, for variants for which no curated evidence is available, interpretation of clinical or biological relevance remains challenging.

It is generally recognized that proteins are the functional units that shape platelet function in both healthy individuals and patients with IPDs [2,8]. Therefore, quantitative high-resolution mass spectrometry (MS)–based proteomics holds a great potential to provide a deeper understanding of the affected molecular mechanisms of both novel and curated genetic variants associated with platelet disorders [9,10]. The first step herein is to assess proteomic alteration in platelets of patients with pathogenic variants in well-curated genes (ie, TIER1 genes). However, thus far, MS–based studies have been restricted to a limited variety of IPDs [9,11,12]. Using label-free quantitative MS–based proteomics, we here investigated the platelet proteomic impact of IPDs with variants in 13 TIER1 genes [3]. We compared these IPDs of different etiologies spanning from early megakaryopoiesis, proplatelet formation, and/or mature platelet function [3].

Overall, we observed a large heterogeneity between IPDs ranging from 1 to 250 differentially abundant proteins. We found limited overlap between IPDs affecting transcription factors and a considerable overlap in affected proteomes between IPDs with genetic variants in cytoskeletal proteins. Furthermore, we demonstrate that protein dynamics clustered across a wide range of IPDs according to cellular function, location, and protein complex membership. Taken together, this study demonstrates that a proteomics point of view provides insight into the molecular backgrounds of platelet (dys) function.

Essentials

- Inherited platelet disorders are a heterogeneous group of rare diseases with various etiologies.
- Mass spectrometry–based proteomic profiling of 13 different IPDs with variants in ISTH TIER1 genes.
- Protein dynamics allow for annotation of platelet alpha granule proteins.
- Mass spectrometry–based proteomics gives insight into the molecular backgrounds of IPDs.

2 | METHODS

2.1 | Study population

The study population consisted of children with a DNA–based IPD diagnosis and affected relatives. The study was approved by the Medical Ethical Review Board of the Erasmus University Medical Center (MEC-2016-218). Patients were included when the following criteria suggested a platelet disorder (1) abnormal bleeding tendency and abnormal platelet indices, (2) prolonged platelet function analyzer (PFA) and/or (3) abnormal light transmission aggregometry (LTA) results, and/or (4) abnormal platelet morphology, combined with a genetic variant in a TIER1 gene as determined by targeted next generation sequencing (tNGS). Affected relatives were also included into our analysis [13]. All participants were included after obtaining written informed consent by legal representatives and patient (if ≥12 years). Owing to the rarity of IPDs, for proteomic analysis, we selected all patients and affected relatives with variants in ISTH TIER1 genes. Additional blood was drawn from healthy, anonymized volunteers in accordance with Dutch regulations and after approval from the Sanquin Ethical Advisory Board. The study was performed according to the Declaration of Helsinki.

2.2 | Hematological assays

Blood was obtained by venipuncture and collected in 9 mL ethylenediaminetetraacetic acid (EDTA) Vacutainer tubes (Becton Dickinson), except for the LTA analysis in which citrated blood was collected. Study participants did not fast before blood draw. Per patient or control, a single tube was used for platelet isolation. In total, 1.8 mg/mL EDTA-blood was used for blood cell indices (Sysmex XN-9100), thrombopoietin (TPO) analysis (in-house enzyme-linked

immunosorbent assay), and citrated blood (0.109 mol/L) was taken for Collagen-ADP (C-ADP) and collagen-epinephrine (C-Epi) cartridges (PFA-200, Siemens), and the LTA PFA was performed on whole blood drawn by venipuncture. Collagen-ADP (C-ADP) and collagen-epinephrine (C-Epi) cartridges were used to measure closure times (seconds) on the PFA-200 (Siemens). Abnormal closure time is defined as >155 seconds.

LTA was performed on a Chrono-Log aggregometer 490 (Stago Benelux) within 20 minutes after venipuncture, following current guidelines [14,15]. In summary, citrated platelet-rich plasma (PRP) was used, obtained by centrifugations at 260 g for 7 minutes at room temperature. A minimal PRP of 150×10^9/L was considered adequate for analysis. Platelet aggregation was assessed using the following agonists and concentrations: adenosine diphosphate (ADP, 5 and if abnormal: 10 μM), archidonic acid (AA, 0.5 mM), collagen (2 and 5 and if abnormal: 10 μg/mL), epinephrine (5 μM and if abnormal epinephrine/ADP mix 1μM/5μM mix), thrombin 1 U/mL (before 2021) and TRAP-6 (30 uM from 2021), and U46619 (4 uM) and Ristocetin (0.31 and 1.25 mg/mL). An abnormal LTA was defined as ≤50% response to ≥1 of the abovementioned agonists or a reversible response defined as a short time >50% response, but no steady state reached >50%.

All PFA and LTA-tests were performed at one central laboratory, "Diagnostic laboratory of hemostasis" Erasmus MC, Rotterdam, NL, according the standardized protocol [14,15].

2.3 | DNA analysis

DNA was isolated from EDTA-blood according to manufacturer's instructions by using the Gentra Puregene kit or the QIAamp DNA Blood Mini Kit (Qiagen, Hilden, Germany). An in-house–developed Ampliseq custom thrombocyte panel (Thermo Fisher Scientific) was used to sequence the coding regions of 73 genes (Supplementary Table S1). Library preparation and sequencing were performed according to manufacturer protocols on a S5 system (Thermo Fisher Scientific). Ion Reporter software (Thermo Fisher Scientific) was used to analyze the genetic sequence data.

2.4 | Sample preparation and mass spectrometry analysis

For MS analysis, a single 9 mL EDTA BD Vacutainer tube was used for platelet isolation. EDTA-blood was centrifuged 2 times for 20 minutes at 120 g to obtain PRP. Next, platelets were isolated by centrifuging for 10 minutes at 2000 g. Platelets were washed 3 times with platelet wash buffer (36 mM citric acid, 103 mM NaCl, 5 mM KCl, 5 mM EDTA, 5.6 mM D-glucose, and 10% (v/v) acid-citrate-dextrose-A [Becton Dickinson, pH 6.5]), and aliquots of 1×10^8 platelets in 25 μL were stored at −80°C until further processing. One aliquot of platelets was lysed in 8 M urea in 100 mM Tris-HCl (pH 8). The protein concentration was determined, and 5 μg of protein was used for sample preparation for MS. Disulphide bonds were reduced with 10 mM dithiotreitol (DTT, Thermo Fisher) for 60 minutes at 20°C, alkylated with 55 mM iodoacetamide (IAM, Thermo Fisher) for 45 minutes at 20°C, and samples were digested overnight at 20°C with MS-grade trypsin Gold (Promega) (in a protein: trypsin ratio of 20:1). Tryptic peptides were desalted and concentrated using Empore-C18 StageTips [16] and eluted with 0.5% (v/v) acetic acid, 80% (v/v) acetonitrile. Samples were dried by SpeedVac and dissolved in 2% acetonitrile, 0.1% trifluoroacetic acid. Tryptic peptides were separated by nanoscale C18 reverse phase chromatography coupled online to an Orbitrap Fusion Tribrid mass spectrometer (Thermo Fisher Scientific) via a nano electrospray ion source (Nanospray Flex Ion Source, Thermo Fisher Scientific). Peptides were loaded on a 20 cm 75 μm 360 μm innerouter diameter fused silica emitter (New Objective) packed in-house with ReproSil-Pur C18-AQ, 1.9 μm resin (Dr Maisch GmbH). The column was installed on a Dionex Ultimate 3000 RSLC nano-System (Thermo Fisher Scientific) using a MicroTee union formatted for 360 μm outer diameter columns (IDEX) and a liquid junction. The spray voltage was set to 2.15 kV. Buffer A was composed of 0.5% acetic acid and buffer B of 0.5% acetic acid, 80% acetonitrile. Peptides were loaded for 17 minutes at 300 nL/minutes at 5% buffer B, equilibrated for 5 minutes at 5% buffer B (17-22 minutes) and eluted by increasing buffer B from 5 to 15% (22-87 minutes) and 15 to 38% (87-147 minutes), followed by a 10 minutes wash to 90% and a 5 minutes regeneration to 5%. Survey scans of peptide precursors from 400 to 1500 m/z were performed in the orbitrap at 120 K resolution with a 4×10^5 ion count target. Tandem MS was performed by isolation with a quadrupole with isolation window 1.6, HCD fragmentation with normalized collision energy of 30, and rapid scan mass spectrometry analysis in the ion trap. The MS2 ion count target was set to 1.5×10^4, and the max injection time was 35 ms. Precursors with charge states 2 to 7 were sampled for MS2. The dynamic exclusion duration was set to 60 seconds with a 10 ppm tolerance around the selected precursor and its isotopes. Monoisotopic precursor selection was turned on. The instrument was run in top speed mode with 3 seconds cycles. The raw MS files and search/identification files obtained with MaxQuant have been deposited in the ProteomeXchange [17] consortium via the PRIDE partner repository [18] with identifier PXD027463. Previously published GFI1B and RUNX1 proteome data were obtained from PXD003912.

2.5 | Data analysis

Raw MS data files were acquired with XCalibur software (Thermo Fisher Scientific) and processed with MaxQuant 1.6.2.10 software [19]. Peptides were searched against the homosapiens Uniprot database (downloaded March 2019, 73 932 entries). An additional database sequence was added to allow for detection of a c-terminal extension event (NP_001447.2.p.Ter26487Serext101) in FLNA [20]. Enzyme specificity was set to trypsin with a maximum of 2 missed cleavages, and carbamidomethylation on cysteine residues was used as fixed modification. The false discovery rate was 0.01 for peptide and protein levels with a minimum length of 7 amino acids. The peptide precursor MS tolerance was set to 10 ppm and fragment ion

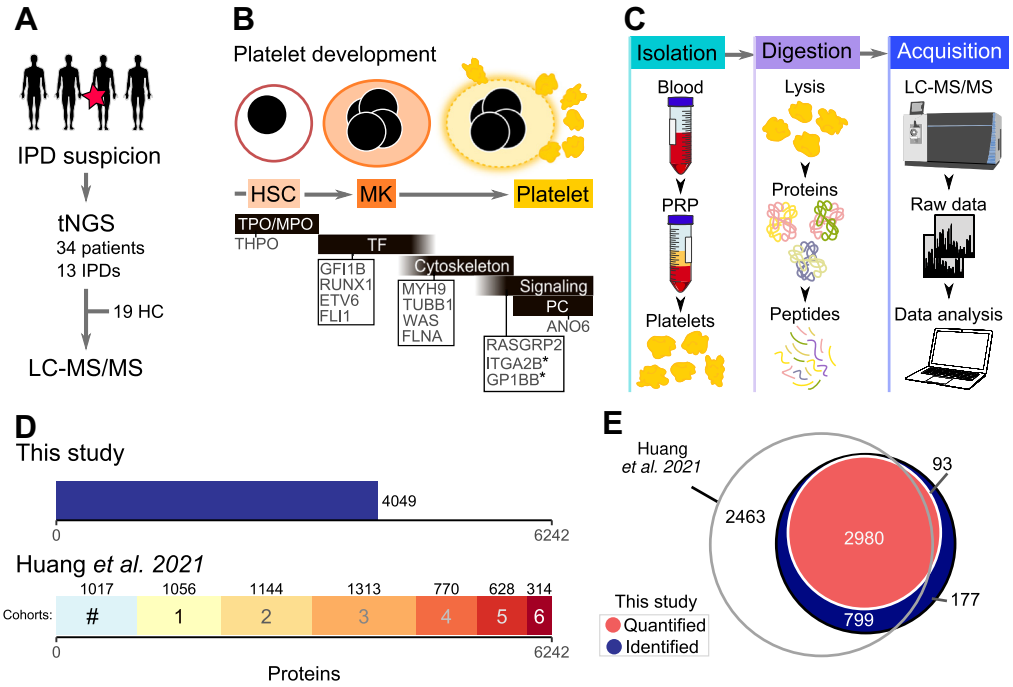

FIGURE 1 Proteomics landscapes of inherited platelet disorders with different etiologies. (A) Flow chart of sample inclusion for spectrometric analysis. (B) Schematic representation of platelet development and categorization of IPDs investigated in this study. *GP1BB and ITGA2B are categorized as signaling molecules, in addition variants in these genes also affect platelet formation. (C) Overview of experimental setup and analysis. Platelets were isolated from whole blood and lysed. Proteins were digested into tryptic peptides and analyzed by quantitative label-free LC-MS/MS. (D) Comparison of the proteins identified in the present study with those identified in the meta-analysis and proteomic study by Huang et al. [11]. Bar colors/numbers indicate amount of studies describing a set of proteins, # indicates proteins directly measured by Huang et al. (E) Overlap of proteins identified by Huang et al. [11] and protein identified (blue) and quantified (coral) in the present study. IPD, inherited platelet disorder; tNGS, targeted next generation sequencing; HC, healthy control.

mass tolerance at 0.6 Dalton. Label-free quantitation (LFQ) was performed with a minimum ratio count of 2 based on unique peptides for quantification. Absolute protein abundances were estimated using intensity-based absolute quantification (iBAQ). MaxQuant output files were loaded in R 4.1.2 for further analysis. Proteins were filtered by "reverse" and "only identified by side," and LFQ intensities were $\log_2$ transformed and iBAQ values were $\log_{10}$ transformed. Proteins were considered quantified based on the presence of 100% valid values in at least one condition. Missing values were imputed by normal distribution (width = 0.3, shift = 1.8). CVs were calculated per protein using all sample intensities. Statistical analysis was performed by comparing each IPD with controls resulting in 13 contrasts using moderated t-tests by using the limma package [21]. To limit potential false positives because of the applied imputation strategy, the results were censored for comparisons in which all conditions contained imputed values. Gene ontology and pathway overrepresentation analyses were performed by using the clusterProfiler package [22]. All *p*-values were corrected for multiple testing using the Benjamini Hochberg method. An adjusted *p* value <.05 was considered statistically significant, for proteomic analyses, an adjusted *p* value <.05 and absolute log-fold change of >1 was considered statistically significant and relevant. To query the data for IPD proxy marker proteins, we defined theoretical profiles for each IPD in which intensities are high for a given IPD and low in all other samples. These profiles were correlated with all quantified proteins, and a selection was made based on an absolute Pearson correlation coefficient threshold of 0.7. Protein dynamics were evaluated by means of weighted gene coexpression network analysis (WGCNA) by using a soft-power of 7 signed network, modules were defined by dynamic tree cut [23]. Correlation between data and disorder specific theoretical protein profiles was performed using Pearson correlation applying a coefficient threshold of 0.7.

3 | RESULTS

3.1 | Patient cohort and platelet proteomes

To study platelet proteomes in IPDs, we included 34 patients and relatives with targeted next generation sequencing (tNGS) variants in 13 TIER1 genes and 19 healthy individuals as controls (Figure 1A, Supplementary Tables S2 and Table). IPDs were categorized into 5 groups according to molecular function: (1) THPO/Mpl signaling: THPO (*N* = 2); (2) transcription regulation: ETV6 (*N* = 2), GFI1B (*N* = 3), FLI1, (*N* = 1), and RUNX1 (*N* = 1); (3) cytoskeleton regulation: MYH9 (*N* = 4), WAS (*N* = 5), FLNA c-terminal extension (*N* = 5), and TUBB1 (*N* = 6); (4) glycoprotein (GP) signaling: GP1BB (*N* = 2), ITGA2B (*N* = 1), RASGRP2

TABLE DNA diagnosis of patients with inherited platelet disorders.

Patient number (DOM)	Family	Gene name	Transcript	Nucleotide	Protein	Molecular consequence	Inheritance
88		*ANO6*	NM_001204803.1	c.1318C>T	p.(Arg440*)	Homozygous nonsense	AR
103	F10	*ETV6*	NM_001987.4	c.1105C>T	p.(Arg369Trp)	Heterozygous missense	AD
104	F10	*ETV6*	NM_001987.4	c.1105C>T	p.(Arg369Trp)	Heterozygous missense	AD
40		*FLI1*	NM_002017.4	c.297del	p.(Met100*)	Heterozygous nonsense	AD
56	F5.1[a]	*FLNA*	NM_001110556.1	c.7941_7942del	p.(*2648Serext*100)	Hemizygous extension	XLR
57	F5.1[a]	*FLNA*	NM_001110556.1	c.7941_7942del	p.(*2648Serext*100)	Heterozygous extension	XLR
111	F5.2[a]	*FLNA*	NM_001110556.1	c.7941_7942del	p.(*2648Serext*100)	Heterozygous extension	XLR
112	F5.2[a]	*FLNA*	NM_001110556.1	c.7941_7942del	p.(*2648Serext*100)	Hemizygous extension	XLR
113	F5.2[a]	*FLNA*	NM_001110556.1	c.7941_7942del	p.(*2648Serext*100)	Hemizygous extension	XLR
19	F3	*GFI1B*	NM_004188.4	c.814+1G>A	p.?	Heterozygous splice site variant	AD
20	F3	*GFI1B*	NM_004188.4	c.814+1G>A	p.?	Heterozygous splice site variant	AD
94	F3	*GFI1B*	NM_004188.4	c.814+1G>A	p.?	Heterozygous splice site variant	AD
66		*GP1BB*	NM_000407.4	c.410T>C	p.(Leu137Pro)	Heterozygous missense	AD
92		*GP1BB*	NM_000407.4	c.281A>G	p.(Asp94Gly)	Homozygous missense	AR
73		*ITGA2B*	NM_000419.3	c.2875G>C	p.(Ala959Pro)	Homozygous missense	AR
10	F2	*MYH9*	NM_002473.4	c.5797C>T	p.(Arg1933*)	Heterozygous nonsense	AD
11	F2	*MYH9*	NM_002473.4	c.5797C>T	p.(Arg1933*)	Heterozygous nonsense	AD
12	F2	*MYH9*	NM_002473.4	c.5797C>T	p.(Arg1933*)	Heterozygous nonsense	AD
43		*MYH9*	NM_002473.4	c.2104C>T	p.(Arg702Cys)	Heterozygous missense	AD
84		*RASGRP2*	NM_001098670.1	c.706C>T	p.(Gln236*)	Homozygous nonsense	AR
86		*RUNX1*	NM_001754.4	c.319C>A	p.(Arg107Ser)	Heterozygous missense	AD
51	F4	*THPO*	NM_009379	c.13+1G>C	p.?	Heterozygous splice site variant	AD
52	F4	*THPO*	NM_009379	c.13+1G>C	p.?	Heterozygous splice site variant	AD
1	F1	*TUBB1*	NM_030773.3	c.721C>T	p.(Arg241Trp)	Heterozygous missense	AD
47	F1	*TUBB1*	NM_030773.3	c.721C>T	p.(Arg241Trp)	Heterozygous missense	AD
48	F1	*TUBB1*	NM_030773.3	c.721C>T	p.(Arg241Trp)	Heterozygous missense	AD
49	F1	*TUBB1*	NM_030773.3	c.721C>T	p.(Arg241Trp)	Heterozygous missense	AD
64	F6	*TUBB1*	NM_030773.3	c.751C>A	p.(Arg251Ser)	Heterozygous missense	AD
65	F6	*TUBB1*	NM_030773.3	c.751C>A	p.(Arg251Ser)	Heterozygous missense	AD

(Continues)

TABLE (Continued)

Patient number (DOM)	Family	Gene name	Transcript	Nucleotide	Protein	Molecular consequence	Inheritance
30		WAS	NM_000377.2	c.399G>C	p.(Glu133Asp)	Hemizygous missense	XLR
77	F8	WAS	NM_000377.2	c.360+3A>T	p.?	Hemizygous splice site variant	XLR
78	F8	WAS	NM_000377.2	c.360+3A>T	p.?	Hemizygous splice site variant	XLR
79	F9	WAS	NM_000377.7	c.173C>A	p.(Pro58His)	Hemizygous missense	XLR
80	F9	WAS	NM_000377.7	c.173C>A	p.(Pro58His)	Hemizygous missense	XLR

AD, autosomal dominant; AR, autosomal recessive; DOM, indicates study patient identifier; F, family member; XLR, X-linked recessive.
[a] 5.1 and 5.2 represent 2 family clusters within a larger pedigree.

(*N* = 1); and (5) procoagulant function: ANO6 (*N* = 1). Figure 1B shows these categories in the context of megakaryopoiesis and platelet function. Note that some variants may affect more than one phenotypic outcome, ie, GP1BB and ITGA2B "signaling" category members also have impact on platelet formation. We applied high-resolution quantitative label-free MS–based proteomics on platelets isolated from peripheral blood (Figure 1C). To assess whether the isolation protocol restricted inclusion of large (>12 fL) platelets, we compared mean platelet volumes (MPV) before and after isolation in all patients and patients with a MPV >12 fL at inclusion (Supplementary Figure S1). This showed that although large platelets (>12 fL) were included, sample MPV was reduced by isolation ($p < .03$). MS analysis resulted in the identification of >58 000 peptides corresponding to 4049 proteins, of which 3073 proteins were reliably quantified (Figure 1D, E). Comparison with a recently published in depth compilation of 7 platelet proteome studies showed that although our dataset contained less protein identifications (Figure 1D), there was a large overlap between proteomes (Figure 1E) [11].

3.2 | Platelet proteomic depth and stability

Plotting the median protein iBAQ intensities (a proxy of absolute quantities) against their ranked abundance showed that these intensities spanned more than 6 orders of magnitude between the most and least abundant proteins. Proteins with established functions in platelets, ie, thymosin beta-4 (TMSB4X), Talin-1 (TLN1), platelet factor 4 (PF4), proplatelet basic protein (PPBP), and thrombospondin-1 (THBS1) [24–26] were highly abundant. Proteins involved with nonsense-mediated mRNA decay (Regulator of nonsense transcripts; UPF2 and Coiled-coil domain-containing protein 9; CCDC9) were measured in the mid-to-low range of detection (Figure 2A). Gene ontology term enrichment on all quantified proteins revealed overrepresentation of platelet associated terms (eg, granules and hemostasis, Figure 2B). Next, we determined the variability and reproducibility of protein quantifications by assessing the coefficient of variation (CV) vs median label-free relative quantification intensities (LFQ). Although an inverse relation between protein intensities and variability was present ($p < 2 \times 10^{16}$, ANOVA; Figure 2C), the highest observed CV was within 20% and the median CV was below 4%. Proteins with high CVs included possible exogenous contaminants (ie, keratins, likely due to sample handling), plasma proteins (immunoglobulins), and cellular contaminations from red and white blood cells (Lactotransferrin, LTF and cytoskeletal associated proteins). Apart from its high relative abundance, TLN1 exhibited the lowest variability [24–26]. Inspection of 6 proteins associated with platelets and/or signaling transduction demonstrated high reproducibility across the measurement range quantiles (Figure 2D), ie, TLN1 (Talin 1) and RABGEF1 (RAB Guanine Nucleotide Exchange Factor 1) which are part of integrin-mediated platelet function and signaling [26–28]. Pro-Platelet Basic Protein (PPBP), a platelet alpha granule constituent [29], syntaxin binding protein 2 (STXBP2), which plays a role in platelet granule secretion [30], and adaptor-related protein

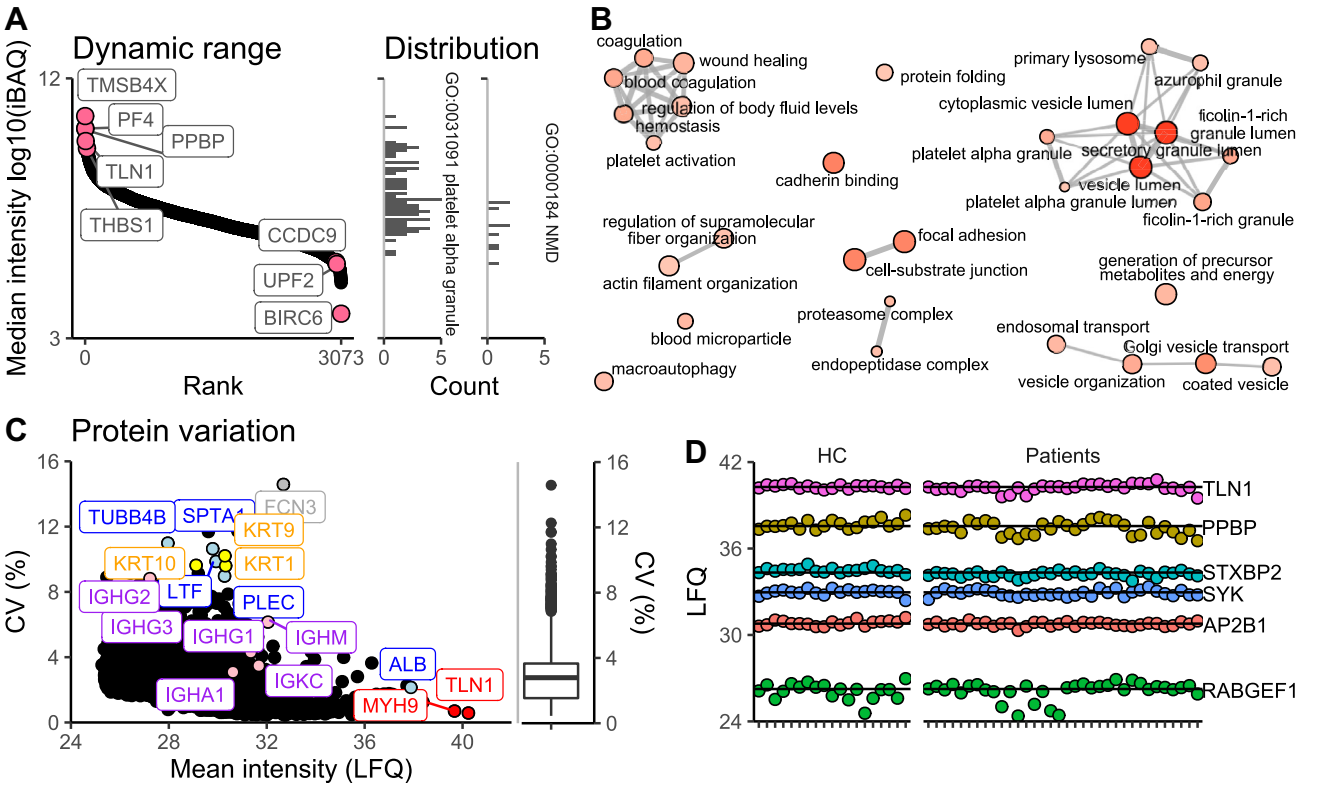

FIGURE 2 Platelet proteomic depth and stability. (A) Dynamic range of quantified proteins (iBAQ intensities are shown). Right panels show intensity distribution of protein annotated with platelet alpha granules (GO:0031091) and nonsense-mediated mRNA decay (NMD, GO:0000184) gene ontology (GO) terms. (B) Gene ontology term enrichment network of all quantified proteins. Node color indicated adjusted P-values, edge width indicates term similarities based on Jaccard's similarity. (C) Scatterplot of coefficients of variance (depicted as CV in %) and mean protein abundances (LFQ). Red labels and dots represent hallmark platelet proteins with highest abundances and inter-individual stability, purple labels and dots show immunoglobulins, yellow dots and labels indicate potential keratin contamination, and teal labels and dots depict proteins with highest coefficients of variance and albumin. (D) LFQ intensities of proteins covering the range of measurement. Solid lines represent mean LFQ intensities. X-axis ticks delimit samples.

complex 2 subunit beta 1 (AP2B1), which is involved in the endosomal vesicle trafficking network [31]. Together, this highlights the overall stability of platelet proteins across IPDs and controls and shows the robustness of label-free MS for comparing protein abundances between platelets of patients with IPDs.

3.3 | Label-free quantitative MS reveals diverging and overlapping IPD proteomes

Comparing platelet proteomes of patients with IPDs and healthy individual resulted in a total of 705 (23% of quantified) significantly differentially abundant proteins (Benjamini Hochberg adjusted $p < .05$ and log-fold change >1) across all IPDs. The impact on platelet proteomes varied greatly between different IPDs (Figure 3A). *TUBB1*, *MYH9*, *WAS*, and *GFI1B* variants induced major proteomic changes, resulting in >200 differentially abundant proteins, whereas the *RASGRP2* variant only impacted the RASGRP2 protein itself. Not all variants translated into measurable differences in corresponding protein abundances (Figure 3B). For genetic variants in transcription factors *ETV6*, *FLI1*, *GFI1B*, *RUNX1*, and growth factor *THPO*, no corresponding proteins could be detected in our data, which was most likely because of their low abundances in circulating platelets. By contrast, MYH9 protein could be detected, although no concordance was observed between the variants in *MYH9* and corresponding protein levels. For *TUBB1*, a minor reduction (0.42 fold) in protein levels could be observed. These findings were not unexpected because all individuals with *MYH9* or *TUBB1* variants were heterozygous. Notably, for *GP1BB* variants, we found that only the homozygous patient (DOM92, Table) exhibited reduced GP1BB protein levels. For *ANO6*, *ITGA2B*, *TUBB1*, and *WAS* variants, we could observe that variants resulted in altered abundances of corresponding proteins. For *FLNA* variant patient platelets, canonical FLNA protein (P21333) abundances did not differ from healthy controls. Because the *FLNA* variant in our study results in a protein with a c-terminal extension, we inspected all detected FLNA peptides. In addition to peptides mapping to the canonical sequence, patient peptides also mapped to the p.Ter26487-Serext101 extension (Figure 3C), thus allowing the identification of this proteoform that is not present in healthy individuals. For the other cases, the protein coverages did not allow for analysis of variant peptides. Owing to the low probability for quantifying THPO (which is produced in the liver) or transcription factor proteins in circulating platelets, we proceeded to interrogate the dataset for the presence of

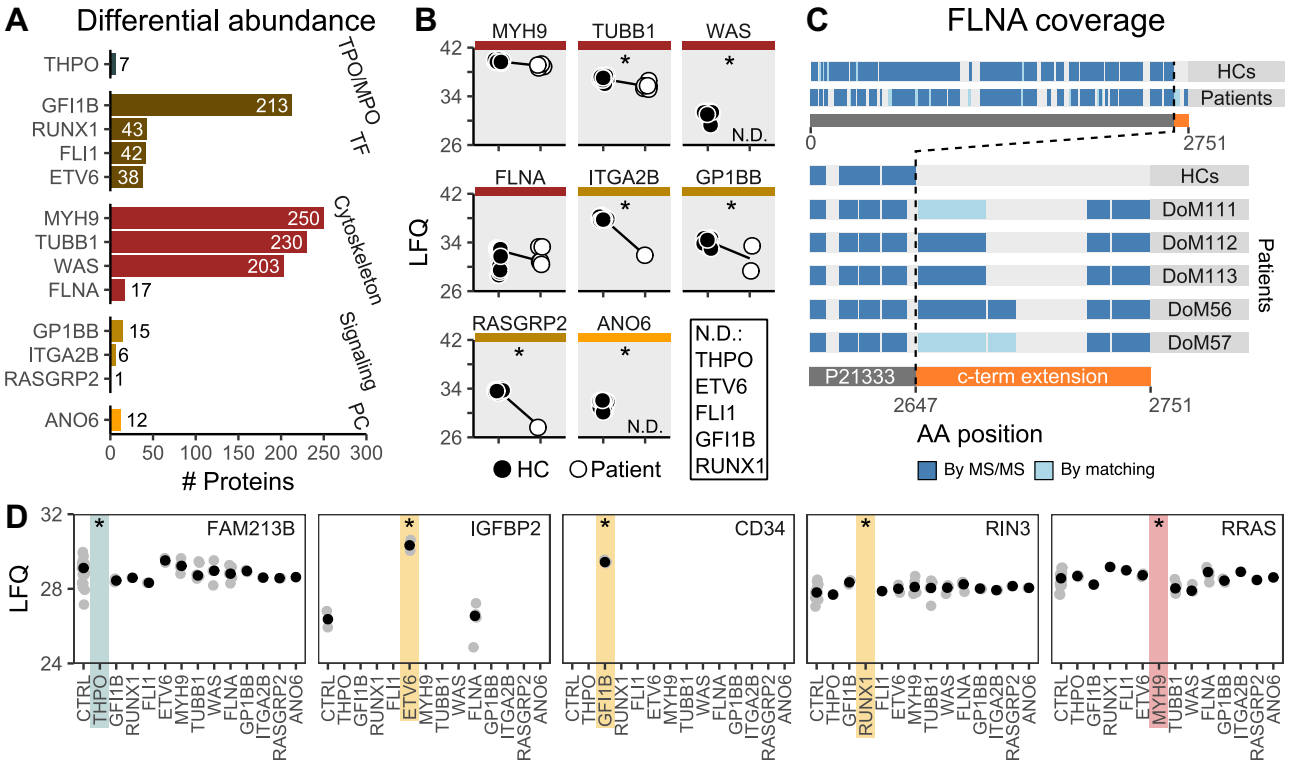

FIGURE 3 Proteomic impact of platelet disorders on platelet proteome. (A) Bar plot of the amount of statistically significant differentially abundant proteins between platelet of inherited platelet disorders and controls per affected TIER1 gene. (B) Dot plot of proteins in which a variant was determined by tNGS. ND, not detected. Closed circles: healthy individuals, and open circles: patients. *Benjamini Hochberg adjusted $p < .05$ and |logFC|>1. (C) Graphic of protein coverage of FLNA (P21333, gray) and the c-terminal extension (orange) in FLNA patients. Zoom shows c-terminal region with peptides mapping to p.Ter2648SerextTer101. Blue represents peptides identified by MS/MS and light blue identified by MaxQuant matching. DOM indicates study patient identifier. (D) Dot plots of putative marker proteins for IPDs for *THPO*, *GFI1B*, *RUNX1*, *ETV6*, and *MYH9*. Selection of proteins that exhibiting absolute correlation coefficients >0.7 with IPD-specific theoretical profiles are shown (see Figure S2). Shaded rectangles indicate for which IPD a protein was considered specific. Gray dots show individual data points; black dots represent medians. *Benjamini Hochberg adjusted $p < .05$ and |logFC|>1.

other IPD-specific proteins that could serve as proxy marker proteins. Correlating platelet proteome data with theoretical specific profiles for these IPDs revealed putative marker proteins for *THPO*, *ETV6*, *GFI1B*, *RUNX1*, and *MYH9* consisting of Prostamide/prostaglandin F synthase (FAM213B), insulin-like growth factor-binding protein 2 (IGFBP2), hematopoietic progenitor cell antigen CD34 (CD34), Ras and Rab interactor 3 (RIN3), and Ras-related protein R-Ras, respectively (Figure 3D and Supplementary Figure S2).

To assess whether different IPDs share common proteomic signatures, we investigated similarities between patient proteomes. Although proteomes were diverse, heatmap visualization indicated overlap between IPDs (Figure 4A). Of the 705 differentially abundant proteins, 301 proteins were shared between multiple IPDs (Supplementary Table S2). Undirected clustering of the differentially abundant proteins showed that GFI1B, RUNX1, and THPO samples clustered together, whereas for other affected genes, this clustering was not as evident (Figure 4B). To further investigate similarities between biological processes, we performed gene ontology enrichment (Figure 4C and Supplementary Table S3). In this analysis, *WAS*, *MYH9*, and *TUBB1* also enriched for similar gene ontology terms. Terms and pathways most enriched in *MYH9* and *TUBB1* samples were mitochondrial associated terms, whereas *ITGA2B* and *GFI1B* samples highly enriched for "alpha granule" associated gene ontology (GO) terms. The latter is in line with the established impact of *GFI1B* deficiency on alpha granules [32].

In addition to gene-centric approaches, we compared the impact of individual variants within a single gene. Both TUBB1 (c.721C>R;R214W, $N = 4$ vs c.751C>A;R251S, $N = 2$) and WAS (c.360 + 3A>T; p.?, $N = 2$ vs c.173C>A; P58H, $N = 2$) variants correlated well with summarized gene ratios (Figure 4D). We extended this by comparing our *GFI1B* and *RUNX1* variant proteomes with independent patient platelet samples from another study (Figures 4E and Supplementary Figure S4) [33]. Between *GFI1B* variants, there was an overlap of 121 proteins (~50%), which included proteins that were previously shown to be affected in *GFI1B* patients (eg, CD34, CXCL5, IQGAP1, and NT5E) [33]. For *RUNX1*, the overlap with the data by van Bergen et al. [33] was considerably less. It should be noted that within the van Bergen study, different RUNX1 variants also showed limited overlap. This indicates that not every variant has the same proteomic impact.

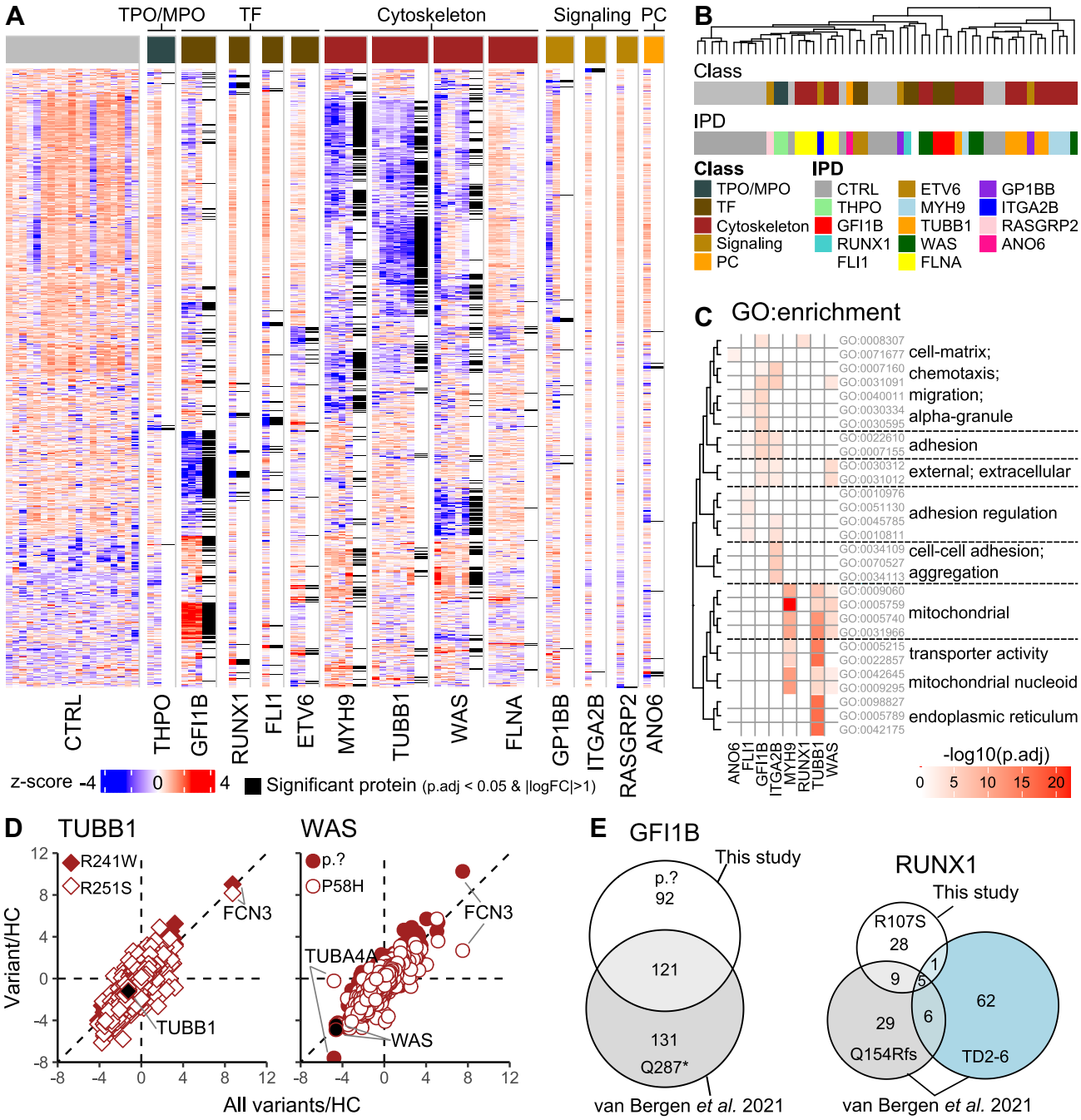

FIGURE 4 Shared and IPD-specific responses and processes. (A) Heatmap of 705 differentially abundant proteins (Benjamini Hochberg adjust $p < .05$ and |logFC|>1) Gradient indicates z-score (low: blue, high: red). Black tiles indicate for which IPD a protein was differentially abundant. Column annotations show IPD class (Teal: TPO/MPO, brown: TF, red: Cytoskeleton, beige: Signaling, orange: PC). (B) Dendrogram of the differentially abundant proteins between IPDs. Color blocks indicate IPD class (Teal: TPO/MPO, brown: TF, red: Cytoskeleton, beige: Signaling, orange: PC) or TIER1 genes (Light green: THPO, Red: GFI1B, Turquoise: RUNX1, White: FLI1, Brown: ETV6, Light Teal MYH9, Orange: TUBB1, Green: WAS, Yellow: FLNA, Purple: GP1BB, Blue: ITGA2B, Light pink: RASGRP2, Pink: ANO6). (C) Tile plot of gene ontology (GO)-enriched terms. Row annotations show GO IDs and high frequency keywords. Lines indicate clusters. Gradient indicates P-adjusted value (low: white, high: red). (D) Scatter plot showing variant specific ratios (y-axis) compared with gene-centric (x-axis) ratios between patients and controls. Diamonds indicate *TUBB1* variants (open: R251S variant, closed: R241W variant). Circles indicate *WAS* variants (open: P58H, closed: p.?). (E) Comparison of proteomic impact of variants of *GFI1B* and *RUNX1* in the present study and van Bergen et al. [33]. Venn-diagram shows the number of overlapping significant proteins. Scatter plot of the median log-fold change of patients vs controls of overlapping proteins.

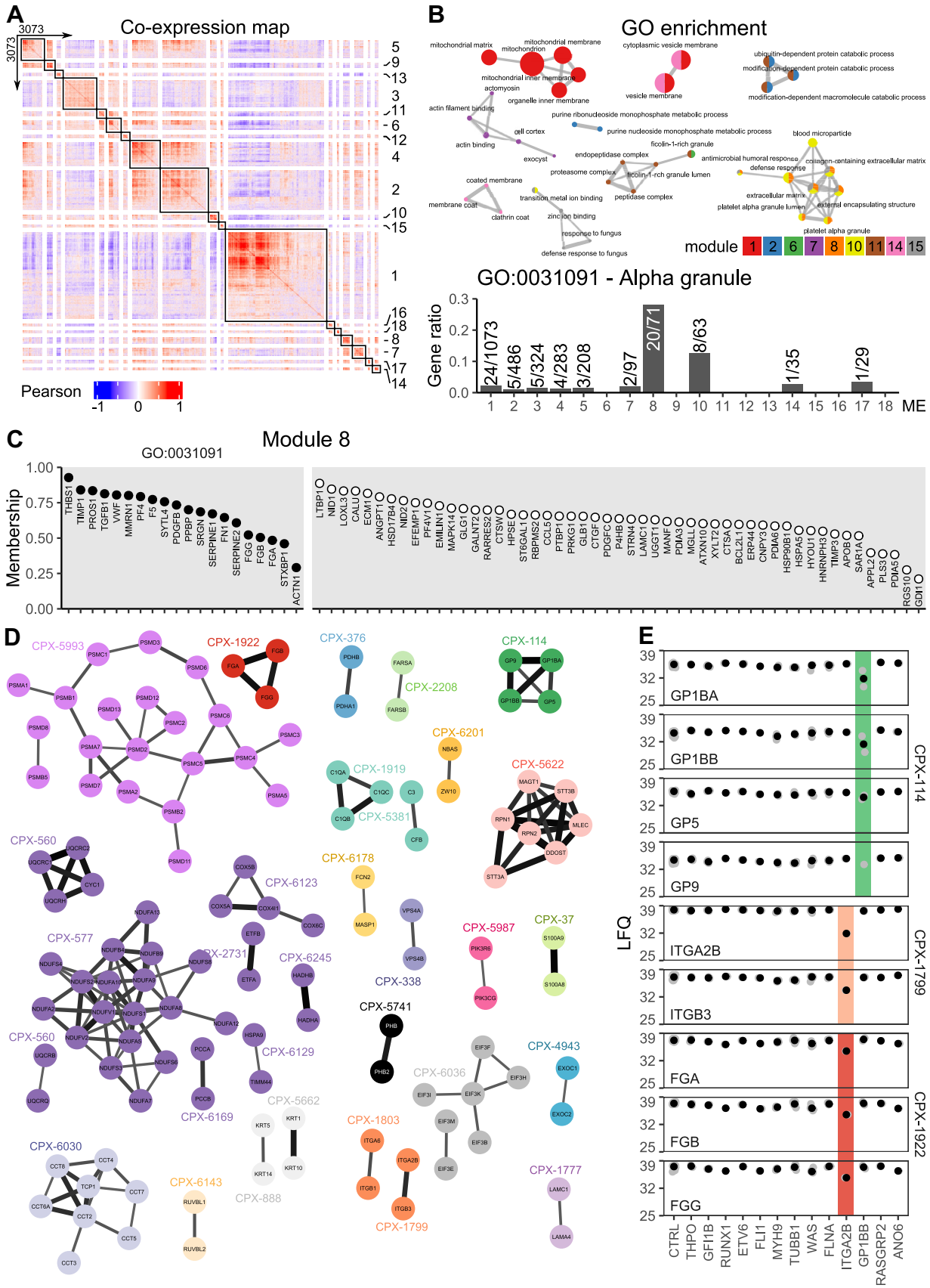

FIGURE 5 Protein dynamics cluster according to IPD and platelet functional aspects. (A) Heatmap of Pearson correlation coefficient of the pairwise comparison of 3073 quantified proteins in this study. Column and row splits are based on WGCNA defined functional modules, indicated with numbers. Color gradient indicated Pearson correlation coefficients (Blue: −1, white: 0, Red: 1). (B) Gene ontology (GO) term enrichment on functional modules. Colors indicate module. Node size indicates amount of proteins a GO term annotation. Edge width indicates

3.4 | Protein dynamics cluster functional aspects and complex memberships

Based on our previous observation that protein dynamics in contrasting conditions can reveal/infer protein function or complex membership [23], we clustered the dynamics of all 3073 quantified proteins using coexpression analysis. WGCNA resulted in 18 modules (MEs) consisting of 23 to 1073 proteins. By combining the WGCNA module allocations and 9 443 329 pairwise Pearson coefficients, we constructed a correlation map of the platelets proteomes in this study (Figure 5A). To determine which biological processes associated with these 18 modules, we performed GO term enrichment (Figure 5B and Supplementary Table S4). This showed that the largest module (ME1) was enriched for mitochondrial and membrane GO terms and that the second largest module (ME2) enriched for catabolic process terms, indicating that a large amount of platelet proteins associate with these functions. Both modules ME8 and ME10 were enriched for the GO term alpha granule proteins, which was greatest for module ME8 ($p < 2.7 \times 10^{-17}$ vs $p < 1.1 \times 10^{-4}$ for ME8 and ME10, respectively). Based on the importance of alpha granules for platelet effector functions, we further investigated module ME8. Proteins in this module with and without alpha granule annotations showed a similar range of module membership scores (Figure 5C), indicating that latter proteins also include putative alpha granule constituents or associated proteins (eg, Latent-transforming growth factor beta-binding protein 1 [LTBP1], angiopoietin-1 [ANGPT1], and C-C motif chemokine 5 [CCL5])[34,35].

By annotating our data using the "Complex Portal" resource [36], we observed that the Pearson coefficient distribution of proteins of known complexes was shifted toward higher positive correlation coefficients ($p < 2 \times 10^{-16}$, Supplementary Figure S3). Next, we selected proteins with correlation coefficients >0.6 and visualized these in a network (Figure 5D). In line with previous reports [37], we found reduced levels of fibrinogen complex (FGA, FGB, FGG; CPX-1922) and integrin alphaIIb-beta3 complex (ITGA2B and ITGB3; CPX-1799) members in the *ITGA2B* variant patient (Figure 5E). We also observed disruption of GP5 complex (GP1BA, GP1BB, GP5 and GP9; CPX-114) in *GP1BB* patients (Figure 5E), which was most pronounced for the homozygous *GP1BB* patient (DOM92). Therefore, these analyses show that harnessing the diversity of IPDs provides a solid basis for inferring platelet protein function and uncovers the current limitations in GO annotations and protein classification.

4 | DISCUSSION

Here, we applied MS–based label-free proteomics to study the impact of IPDs on the platelet proteome. In contrast to current literature on IPDs using MS–based proteomics [37–39], our study includes a wide range of IPDs that enables the concurrent investigation of proteomic effects of platelet disorders with different etiologies. We found that the phenotypical heterogeneity between IPDs is also present at the proteome level. Although ~1/3 of the platelet proteome was altered across all IPDs in our study, most IPDs exhibited a limited impact on the platelet proteome.

The largest effects were because of the variants in cytoskeletal proteins, which altered up to ~8% of quantified proteins. MYH9, WAS, and TUBB1 are associated with proplatelet formation [40], which may explain their large impact. By contrast, *FLNA* resulted in only 17 altered protein abundances. Although *FLNA* variants may either impact platelet development or activation [41], the *FLNA c-terminal extension* genetic variant in our study was previously associated with enhanced effector functions rather than disrupted platelet formation [20]. In a recent study, the proteomic effects of variants in *GFI1B*, *RUNX1*, and *GATA2* transcription factors were assessed [33]. In line with this study, we show that the *GFI1B* variant had a larger impact than other transcription factor defects. GFI1B deficiency is well established regarding its effects on the biosynthesis of protein-rich platelet alpha granules [42]. By contrast, deficiencies in *RUNX1* and *FLI1* were described to impact dense granules [43,44], which are low in protein content. Furthermore, ETV6 was recently suggested to play a role in terminal megakaryopoiesis, although no large phenotypic effects were observed other than thrombocytopenia [45]. This distinction between monogenetic to mono/oligoproteomic vs polyproteomic effects implies that the extent of anomalies in a platelet proteome is not necessarily indicative of disease severity. Illustrative of this, in a recent study that included 38 patients from 9 families with *TUBB1* variants (with 230 significant proteins in our study), no severe bleeding phenotype was observed [46]. By contrast, Glanzmann thrombasthenia (*ITGA2B*, 6 significant proteins in our study) is associated with a severe bleeding phenotype [47]. In addition, the impact on the platelet proteome differed between homozygous vs heterozygous variant carriers, illustrated by the *GP1BB* patients in which GP-complex proteins were less affected in the heterozygous individual.

The platelet proteomic profiles of the diverse array of IPDs incorporated in our study provided a fundament to study inter-protein dynamics that underly platelet functions. This allowed us to identify disruption of protein complexes. In Glanzmann thrombasthenia platelets, we observed reduced ITGA2B and ITGB3 abundances. Consequently, we also found fibrinogen (FGA, FGB, and FGG) in reduced amounts in line with established findings that this complex is internalized from the circulation by these integrin receptors [37,48].

Moreover, coexpression clustering combined with GO term analysis highlighted distinct protein groups and enriched processes. The largest set of highly correlating proteins described mitochondrial

GO term similarities based on Jaccard's similarity. Bar plot shows distribution of protein with alpha granule annotation over all modules as gene ratios. (C) Dot plots showing membership scores of proteins in module ME8. Filled circles indicate annotated alpha granule proteins, and open circle indicates protein without alpha granule annotation. (D) Network of protein annotated as complex members based on the EBI "Complex Portal" resource. Edges width reflect Pearson correlation coefficients. (E) Dot plots showing protein intensities of protein in complexes CPX-114 (GP5 complex), CPX-1799 (Integrin alphaIIb-beta3 complex), and CPX-1922(fibrinogen complex). Black dots represent median LFQ intensities, and gray dot represents patient LFQ intensity.

processes, which emphasizes the integral role mitochondria play in platelet metabolism and function [49]. The dynamics summarized by module ME8 highly enriched for alpha granule annotated proteins (Figure 5). Apart from well-known platelet alpha granule constituents (eg, Thrombospondin-1, von Willebrand factor, and platelet factor 4), this module included proteins that despite lack of previous annotation have been associated with alpha granules. Using MS analysis to investigate alpha granule enriched subcellular fractions, Maynard et al. [50] previously identified ANGPT1, CCL5, and CTFG as putative alpha granule constituents, which in our analysis were all members of ME8. In another study, these authors convincingly showed that latent-transforming growth factor beta-binding protein 1 (LTBP1) is present within platelet alpha granules [51]. Therefore, the dynamics in module ME8 are indicative of alpha granule-associated proteins.

Our study has limitations. Our centrifugation based isolation protocol, although not excluding large platelets, exhibited a bias toward platelets with a smaller volume. Although the study population consisted of children and affected relatives, all control samples were obtained from adults. Therefore, apart from IPD impact age may have influenced platelet proteomes. Depending on the IPD, we were able to include a limited amount of individuals, which impacts the findings we present. A shortcoming of our approach is the relatively limited recovery of low-abundant proteins because of constraints in the dynamic range of current untargeted MS methods. In cases of low abundance, a protein may be below the detection limit (eg, transcription factors). In addition, proteins that have functions during platelet formation in the bone marrow may also be absent in mature platelets. Targeted proteomics may partially overcome this and has proven to be reliable in accuracy and quantification. However, the amount of simultaneously measured target proteins is substantially less than in discovery based untargeted MS [38]. Recently, Malchow et al. [52] applied targeted MS to quantify 99 IPD-related proteins. To expand on this, the platelet proteomes we present in this study may be used as a guide for refinement. For instance, for IPDs that lacked a match between a genetic variation and the corresponding protein, putative marker proteins could be targeted to identify these disorders (eg, RIN3 for *RUNX1* and CD34 for *GFI1B*). Although needing further validation, eg, the observation of enhanced platelet CD34 levels in the GFI1B variant is in line with multiple other studies in GFI1B patients [53,54]. Furthermore, it should be noted that applying MS–based proteomics is more suited to elucidate thrombocytopathy rather than thrombocytopenia, in which platelet numbers are affected but not their composition.

In conclusion, in this study, we demonstrated a proteomics perspective that complements DNA–based IPD diagnosis. Moreover, by integrating disorders that span the genetic landscape of platelet development, we dissected biological contexts of protein alterations that may aid in the development of deeper insights into the molecular backgrounds of IPDs and platelet biology in general.

ACKNOWLEDGMENTS

The work presented here was supported by the Landsteiner Foundation for Blood Transfusion Research [LSBR-1517 to M.v.d.B., LSBR-1923 to M.v.d.B. and A.J.H]. We acknowledge all the patients and family members who contributed to this research. The authors would like to thank the people from the research facility of Sanquin for helping with isolation of platelets.

AUTHOR CONTRIBUTIONS

A.J.H., E.J.H., I.C.K., A.B.M., M.v.d.B., M.d.H., M.H.C., C.M.Z., and C.S.B.V. designed the study. A.J.H. and I.C.K. analyzed data, supervised research, and wrote the manuscript. I.C.K., F.P.J.A., C.v.d.Z., L.P., and K.v.L. performed the experiments. K.v.L. and R.S. analyzed the DNA data. E.J.H. acquired patient data, analyzed data, and wrote the manuscript. A.J.H., A.B.M., M.H.C., M.d.H., and M.v.d.B. supervised research. All authors approved the final version of the manuscript.

DECLARATION OF COMPETING INTERESTS

The authors declare no conflict of interest.

DATA SHARING STATEMENT

All raw MS files and search/identification files are available via ProteomeXchange with identifier PXD027463.

REFERENCES

[1] Golebiewska EM, Harper MT, Williams CM, Savage JS, Goggs R, von Mollard GF, Poole AW. Syntaxin 8 regulates platelet dense granule secretion, aggregation, and thrombus stability. *J Biol Chem*. 2015;290:1536–45. https://doi.org/10.1074/jbc.M114.602615

[2] Gianazza E, Brioschi M, Baetta R, Mallia A, Banfi C, Tremoli E. Platelets in healthy and disease states: from biomarkers discovery to drug targets identification by proteomics. *Int J Mol Sci*. 2020;21:1–44. https://doi.org/10.3390/ijms21124541

[3] Lentaigne C, Freson K, Laffan MA, Turro E, Ouwehand WH. BRIDGE-BPD Consortium and the ThromboGenomics Consortium. Inherited platelet disorders: toward DNA-based diagnosis. *Blood*. 2016;127:2814–23. https://doi.org/10.1182/blood-2016-03-378588

[4] Downes K, Megy K, Duarte D, Vries M, Gebhart J, Hofer S, Shamardina O, Deevi SVV, Stephens J, Mapeta R, Tuna S, Hasso NA, Besser MW, Cooper N, Daugherty L, Gleadall N, Greene D, Haimel M, Martin H, Papadia S, et al. Diagnostic high-throughput sequencing of 2396 patients with bleeding, thrombotic, and platelet disorders. *Blood*. 2019;134:2082–91. https://doi.org/10.1182/blood.2018891192

[5] Bastida JM, Lozano ML, Benito R, Janusz K, Palma-Barqueros V, Del Rey M, Hernández-Sánchez JM, Riesco S, Bermejo N, González-García H, Rodriguez-Alén A, Aguilar C, Sevivas T, López-Fernández MF, Marneth AE, van der Reijden BA, Morgan NV, Watson SP, Vicente V, Hernández-Rivas JM, et al. Introducing high-throughput sequencing into mainstream genetic diagnosis practice in inherited platelet disorders. *Haematologica*. 2018;103:148–62. https://doi.org/10.3324/haematol.2017.171132

[6] Megy K, Downes K, Morel-Kopp MC, Bastida JM, Brooks S, Bury L, Leinoe E, Gomez K, Morgan NV, Othman M, Ouwehand WH, Botero JP, Rivera J, Schulze H, Trégouët D-A, Freson K. Gold-Variants, a resource for sharing rare genetic variants detected in bleeding, thrombotic, and platelet disorders: communication from the ISTH SSC subcommittee on genomics in thrombosis and hemostasis. *J Thromb Haemost*. 2021;19:2612–7. https://doi.org/10.1111/jth.15459

[7] 100,000 Genomes Project Pilot Investigators, Smedley D, Smith KR, Martin A, Thomas EA, McDonagh EM, Cipriani V, Ellingford JM, Arno G, Tucci A, Vandrovcova J, Chan G, Williams HJ, Ratnaike T,

Wei W, Stirrups K, Ibanez K, Moutsian L, Wielscher M, Need A, et al. 100,000 genomes pilot on rare-disease diagnosis in health care—preliminary report. *N Engl J Med*. 2021;385:1868–80. https://doi.org/10.1056/NEJMoa2035790

[8] Stalker TJ, Newman DK, Peisong M, Wannemacher KM, Brass LF. Platelet signaling. *Handb Exp Pharmacol*. 2012;210:59–85. https://doi.org/10.1007/978-3-642-29423-5

[9] Burkhart JM, Vaudel M, Gambaryan S, Radau S, Walter U, Martens L, Geiger J, Sickmann A, Zahedi RP. The first comprehensive and quantitative analysis of human platelet protein composition allows the comparative analysis of structural and functional pathways. *Blood*. 2012;120:e73–82. https://doi.org/10.1182/blood-2012-04-416594

[10] McRedmond JP, Park SD, Reilly DF, Coppinger JA, Maguire PB, Shields DC, Fitzgerald DJ. Integration of proteomics and genomics in platelets: a profile of platelet proteins and platelet-specific genes. *Mol Cell Proteomics*. 2004;3:133–44. https://doi.org/10.1074/mcp.M300063-MCP200

[11] Huang J, Swieringa F, Solari FA, Provenzale I, Grassi L, De Simone I, Baaten CCFMJ, Cavill R, Sickmann A, Frontini M, Heemskerk JWM. Assessment of a complete and classified platelet proteome from genome-wide transcripts of human platelets and megakaryocytes covering platelet functions. *Sci Rep*. 2021;11:12358. https://doi.org/10.1038/s41598-021-91661-x

[12] McRedmond JP, Park SD, Reilly DF, Coppinger JA, Maguire PB, Shields DC, Fitzgerald DJ. Integration of proteomics and genomics in platelets.: a profile of platelet proteins and platelet-specific genes. *Mol Cell Proteomics*. 2004;3:133–44. https://doi.org/10.1074/mcp.M300063-MCP200

[13] Richards S, Aziz N, Bale S, Bick D, Das S, Gastier-Foster J, Grody WW, Hegde M, Lyon E, Spector E, Voelkerding K, Rehm HL, ACMG Laboratory Quality Assurance Committee. Standards and guidelines for the interpretation of sequence variants: a joint consensus recommendation of the American College of Medical Genetics and Genomics and the Association for Molecular Pathology. *Genet Med*. 2015;17:405–24. https://doi.org/10.1038/gim.2015.30

[14] Cattaneo M, Cerletti C, Harrison P, Hayward CPM, Kenny D, Nugent D, et al. Recommendations for the standardization of light transmission aggregometry: a consensus of the working party from the platelet physiology subcommittee of SSC/ISTH. *J Thromb Haemost*. 2013;11:1183–9. https://doi.org/10.1111/jth.12231.

[15] Munnix ICA, van Oerle R, Verhezen P, Kuijper P, Hackeng CM, Hopman-Kerkhoff HIJ, et al. Harmonizing light transmission aggregometry in the Netherlands by implementation of the SSC-ISTH guideline. *Platelets*. 2021;32:516–23. https://doi.org/10.1080/09537104.2020.1771549.

[16] Rappsilber J, Ishihama Y, Mann M. Stop and go extraction tips for matrix-assisted laser desorption/ionization, nanoelectrospray, and LC/MS sample pretreatment in proteomics. *Anal Chem*. 2003;75:663–70. https://doi.org/10.1021/ac026117i

[17] Deutsch EW, Csordas A, Sun Z, Jarnuczak A, Perez-Riverol Y, Ternent T, Campbell DS, Bernal-Llinares M, Okuda S, Kawano S, Moritz RL, Carver JJ, Wang M, Ishihama Y, Bandeira N, Hermjakob H, Vizcaíno JA. The ProteomeXchange Consortium in 2017: supporting the cultural change in proteomics public data deposition. *Nucleic Acids Res*. 2017;45:D1100–6. https://doi.org/10.1093/nar/gkw936

[18] Perez-Riverol Y, Csordas A, Bai J, Bernal-Llinares M, Hewapathirana S, Kundu DJ, Inuganti A, Griss J, Mayer G, Eisenacher M, Pérez E, Uszkoreit J, Pfeuffer J, Sachsenberg T, Yilmaz S, Tiwary S, Cox J, Audain E, Walzer M, Jarnuczak AF. The PRIDE database and related tools and resources in 2019: improving support for quantification data. *Nucleic Acids Res*. 2019;47:D442–50. https://doi.org/10.1093/nar/gky1106

[19] Neuhauser N, Michalski A, Scheltema RA, Olsen JV, Mann M. Andromeda : a peptide search engine integrated into the MaxQuant environment. *J Proteome Res*. 2011;10:1794–805. https://doi.org/10.1021/pr101065j

[20] Berrou E, Adam F, Lebret M, Planche V, Fergelot P, Issertial O, Coupry I, Bordet JC, Nurden P, Bonneau D, Colin E, Goizet C, Rosa JP, Bryckaert M. Gain-of-function mutation in filamin A potentiates platelet integrin α IIb β 3 activation. *Arterioscler Thromb Vasc Biol*. 2017;37:1087–97. https://doi.org/10.1161/ATVBAHA.117.309337

[21] Phipson B, Lee S, Majewski IJ, Alexander WS, Smyth G. Robust hyperparameter estimation protects against hypervariable genes and improves power to detect differential expression. *Ann Appl Stat*. 2016;10:946–63. https://doi.org/10.1214/16-AOAS920

[22] Yu G, Wang LG, Han Y, He QY. ClusterProfiler: an R package for comparing biological themes among gene clusters. *Omics*. 2012;16:284–7. https://doi.org/10.1089/omi.2011.0118

[23] Langfelder P, Horvath S. WGCNA: an R package for weighted correlation network analysis. *BMC Bioinf*. 2008;9:559. https://doi.org/10.1186/1471-2105-9-559

[24] Scheller I, Beck S, Göb V, Gross C, Neagoe RAI, Aurbach K, Bender M, Stegner D, Nagy Z, Nieswandt B. Thymosin β4 is essential for thrombus formation by controlling the G-actin/F-actin equilibrium in platelets. *Haematologica*. 2022;107:2846–58. https://doi.org/10.3324/haematol.2021.278537

[25] Wijten P, van Holten T, Woo LL, Bleijerveld OB, Roest M, Heck AJR, Scholten A. High precision platelet releasate definition by quantitative reversed protein profiling-brief report. *Arterioscler Thromb Vasc Biol*. 2013;33:1635–8. https://doi.org/10.1161/ATVBAHA.113.301147

[26] Lagarrigue F, Paul DS, Gingras AR, Valadez AJ, Sun H, Lin J, Cuevas MN, Ablack JN, Lopez-Ramirez MA, Bergmeier W, Ginsberg MH. Talin-1 is the principal platelet Rap1 effector of integrin activation. *Blood*. 2020;136:1180–90. https://doi.org/10.1182/blood.2020005348

[27] Petrich BG, Marchese P, Ruggeri ZM, Spiess S, Weichert RAM, Ye F, Tiedt R, Skoda RC, Monkley SJ, Critchley DR, Ginsberg MH. Talin is required for integrin-mediated platelet function in hemostasis and thrombosis. *J Exp Med*. 2007;204:3103–11. https://doi.org/10.1084/jem.20071800

[28] Stefanini L, Bergmeier W. RAP GTPases and platelet integrin signaling. *Platelets*. 2019;30:41–7. https://doi.org/10.1080/09537104.2018.1476681

[29] El-Gedaily A, Schoedon G, Schneemann M, Schaffner A. Constitutive and regulated expression of platelet basic protein in human monocytes. *J Leukoc Biol*. 2004;75:495–503. https://doi.org/10.1189/jlb.0603288

[30] al Hawas R, Ren Q, Ye S, Karim ZA, Filipovich AH, Whiteheart SW. Munc18b/STXBP2 is required for platelet secretion. *Blood*. 2012;120:2493–500. https://doi.org/10.1182/blood-2012-05-430629

[31] Lee H, Chae S, Park J, Bae J, Go E-B, Kim S-J, Kim H, Hwang D, Lee S-W, Lee S-Y. Comprehensive proteome profiling of platelet identified a protein profile predictive of responses to an antiplatelet agent sarpogrelate. *Mol Cell Proteomics*. 2016;15:3461–72. https://doi.org/10.1074/mcp.M116.059154

[32] Noris P, Pecci A. Hereditary thrombocytopenias: a growing list of disorders. *Hematology Am Soc Hematol Educ Program*. 2017;2017:385–99. https://doi.org/10.1182/asheducation-2017.1.385

[33] van Bergen MGJM, Marneth AE, Hoogendijk AJ, van Alphen FPJ, van den Akker E, Laros-Van Gorkom BAP, Hoeks M, Simons A, De Munnik SA, Janssen JJWM, Martens JHA, Jansen JH, Meijer AB, van der Reijden BA. Specific proteome changes in platelets from individuals with GATA1-, GFI1B-, and RUNX1-linked bleeding disorders. *Blood*. 2021;138:86–90. https://doi.org/10.1182/blood.2020008118

[34] Machlus KR, Johnson KE, Kulenthirarajan R, Forward JA, Tippy MD, Soussou TS, El-Husayni SE, Wu SK, Wang S, Watnick RS, Italiano JE Jr, Battinelli EM. CCL5 derived from platelets increases megakaryocyte proplatelet formation. *Blood*. 2016;127:921–6. https://doi.org/10.1182/blood-2015-05

[35] Chanzu H, Lykins J, Wigna-Kumar S, Joshi S, Pokrovskaya I, Storrie B, Pejler G, Wood JP, Whiteheart SW. Platelet α-granule cargo packaging and release are affected by the luminal proteoglycan, serglycin. *J Thromb Haemost*. 2021;19:1082–95. https://doi.org/10.1111/jth.15243

[36] Combe CW, Sivade MD, Hermjakob H, Heimbach J, Meldal BHM, Micklem G, Orchard S, Rappsilber J. ComplexViewer: visualization of curated macromolecular complexes. *Bioinformatics*. 2017;33:3673–5. https://doi.org/10.1093/bioinformatics/btx497

[37] Loroch S, Trabold K, Gambaryan S, Reiß C, Schwierczek K, Fleming I, Sickmann A, Behnisch W, Zieger B, Zahedi RB, Walter U, Jurk K. Alterations of the platelet proteome in type I Glanzmann thrombasthenia caused by different homozygous delG frameshift mutations in ITGA2B. *Thromb Haemost*. 2017;117:556–69. https://doi.org/10.1160/TH16-07-0515

[38] Solari FA, Mattheij NJA, Burkhart JM, Swieringa F, Collins PW, Cosemans JMEM, Sickmann A, Heemskerk JWM, Zahedi RP. Combined quantification of the global proteome, phosphoproteome, and proteolytic cleavage to characterize altered platelet functions in the human Scott syndrome. *Mol Cell Proteomics*. 2016;15:3154–69. https://doi.org/10.1074/mcp.M116.060368

[39] Winkler W, Zellner M, Diestinger M, Babeluk R, Marchetti M, Goll A, Zehetmayer S, Bauer P, Rappold E, Miller I, Roth E, Allmaier G, Oehler R. Biological variation of the platelet proteome in the elderly population and its implication for biomarker research. *Mol Cell Proteomics*. 2008;7:193–203. https://doi.org/10.1074/mcp.M700137-MCP200

[40] Ghalloussi D, Dhenge A, Bergmeier W. New insights into cytoskeletal remodeling during platelet production. *J Thromb Haemost*. 2019;17:1430–9. https://doi.org/10.1111/jth.14544

[41] Rosa JP, Raslova H, Bryckaert M. Filamin a: key actor in platelet biology. *Blood*. 2019;134:1279–88. https://doi.org/10.1182/blood.2019000014

[42] Stevenson WS, Morel-Kopp MC, Chen Q, Liang HP, Bromhead CJ, Wright S, Turakulov R, Ng AP, Roberts AW, Bahlo M, Ward CM. GFI1B mutation causes a bleeding disorder with abnormal platelet function. *J Thromb Haemost*. 2013;11:2039–47. https://doi.org/10.1111/jth.12368

[43] Glembotsky AC, Bluteau D, Espasandin YR, Goette NP, Marta RF, Oyarzun CPM, Korin L, Lev PR, Laguens RP, Molinas FC, Raslova H, Heller PG. Mechanisms underlying platelet function defect in a pedigree with familial platelet disorder with a predisposition to acute myelogenous leukemia: potential role for candidate RUNX1 targets. *J Thromb Haemost*. 2014;12:761–72. https://doi.org/10.1111/jth.12550

[44] Saultier P, Vidal L, Canault M, Bernot D, Falaise C, Pouymayou C, Bordet J-C, Saut N, Rostan A, Baccini V, Peiretti F, Favier M, Lucca P, Deleuze J-F, Olaso R, Boland A, Morange PE, Gachet C, Malergue F, Fauré S, et al. Macrothrombocytopenia and dense granule deficiency associated with FLI1 variants: ultrastructural and pathogenic features. *Haematologica*. 2017;102:1006–16. https://doi.org/10.3324/haematol.2016.153577

[45] Melazzini F, Palombo F, Balduini A, De Rocco D, Marconi C, Noris P, Gnan C, Pippucci T, Bozzi V, Faleschini M, Barozzi S, Doubek M, Di Buduo CA, Kozubik KS, Radova L, Loffredo G, Pospisilova S, Alfano C, Seri M, Balduini CL, et al. Clinical and pathogenic features of ETV6-related thrombocytopenia with predisposition to acute lymphoblastic leukemia. *Haematologica*. 2016;101:1333–42. https://doi.org/10.3324/haematol.2016.147496

[46] Palma-Barqueros V, Bury L, Kunishima S, Lozano ML, Rodríguez-Alen A, Revilla N, Bohdan N, Padilla J, Fernández-Pérez MP, de la Morena-Barrio ME, Marín-Quilez A, Benito R, López-Fernández MF, Marcellini S, Zamora-Cánovas A, Vicente V, Martínez C, Gresele P, Bastida JM, Rivera J. Expanding the genetic spectrum of TUBB1-related thrombocytopenia. *Blood Adv*. 2021;5:5453–67. https://doi.org/10.1182/bloodadvances.2020004057

[47] Botero JP, Lee K, Branchford BR, Bray PF, Freson K, Lambert MP, Luo M, Mohan S, Ross JE, Bergmeier W, Di Paola J. Glanzmann thrombasthenia: genetic basis and clinical correlates. *Haematologica*. 2020;105:888–94. https://doi.org/10.3324/haematol.2018.214239

[48] Disdier M, Legrand C, Bouillot C, Dubernard V, Pidard D, Nurden AT. Quantitation of platelet fibrinogen and thrombospondin in Glanzmann's thrombasthenia by electroimmunoassay. *Thromb Res*. 1989;53:521–33. https://doi.org/10.1016/0049-3848(89)90142-4

[49] Melchinger H, Jain K, Tyagi T, Hwa J. Role of platelet mitochondria: life in a nucleus-free zone. *Front Cardiovasc Med*. 2019;6:153. https://doi.org/10.3389/fcvm.2019.00153

[50] Maynard DM, Heijenen HDG, Horne MK, White JG, Gahl WA. Proteomic analysis of platelet α-granules using mass spectrometry. *J Thromb Haemost*. 2007;5:1945–55. https://doi.org/10.1111/j.1538-7836.2007.02690.x

[51] Maynard DM, Heijnen HFG, Gahl WA, Gunay-Aygun M. The α-granule proteome: novel proteins in normal and ghost granules in gray platelet syndrome. *J Thromb Haemost*. 2010;8:1786–96. https://doi.org/10.1111/j.1538-7836.2010.03932.x

[52] Malchow S, Loosse C, Sickmann A, Lorenz C. Quantification of cardiovascular disease biomarkers in human platelets by targeted mass spectrometry. *Proteomes*. 2017;5:31. https://doi.org/10.3390/proteomes5040031

[53] Rabbolini DJ, Morel-Kopp MC, Chen Q, Gabrielli S, Dunlop LC, Chew LP, Blair N, Brighton TA, Singh N, Ng AP, Ward CM, Stevenson WS. Thrombocytopenia and CD34 expression is decoupled from α-granule deficiency with mutation of the first growth factor-independent 1B zinc finger. *J Thromb Haemost*. 2017;15:2245–58. https://doi.org/10.1111/jth.13843

[54] Palareti G, Legnani C, Cosmi B, Antonucci E, Erba N, Poli D, Testa S, Tosetto A. Comparison between different D-Dimer cutoff values to assess the individual risk of recurrent venous thromboembolism: analysis of results obtained in the DULCIS study. *Int J Lab Hematol*. 2016;38:42–9. https://doi.org/10.1111/ijlh.12426

SUPPLEMENTARY MATERIAL

The online version contains supplementary material available at https://dx.doi.org/10.1016/j.jtha.2022.11.021.

SUPPLEMENTARY FIGURE S1 MPV levels on arrival of blood in our laboratory and after platelet isolation for entire patient population (left panel) and (right panel) of patients with MPV > 12 fl at inclusion.

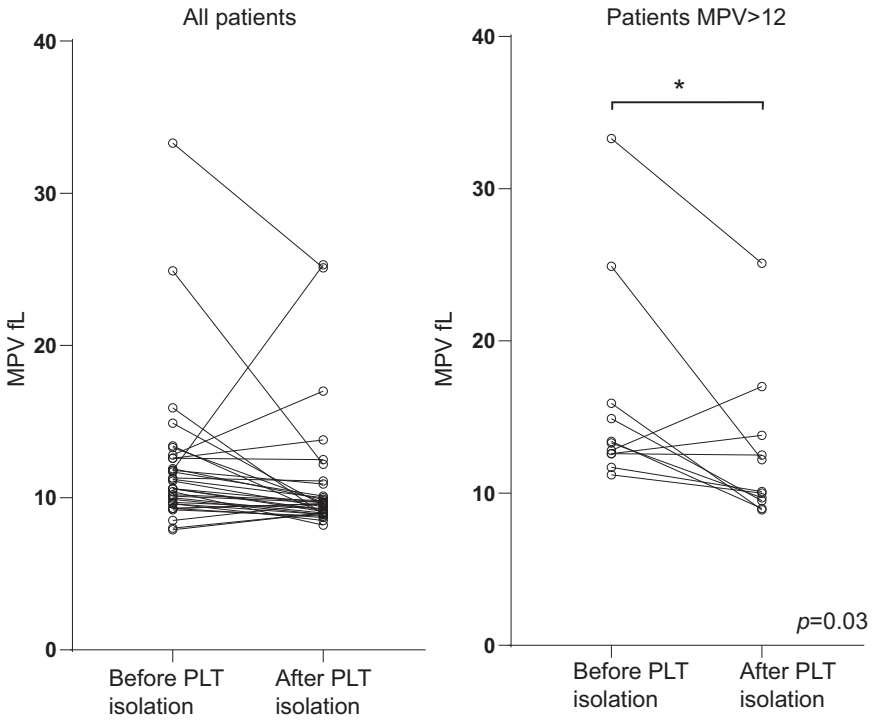

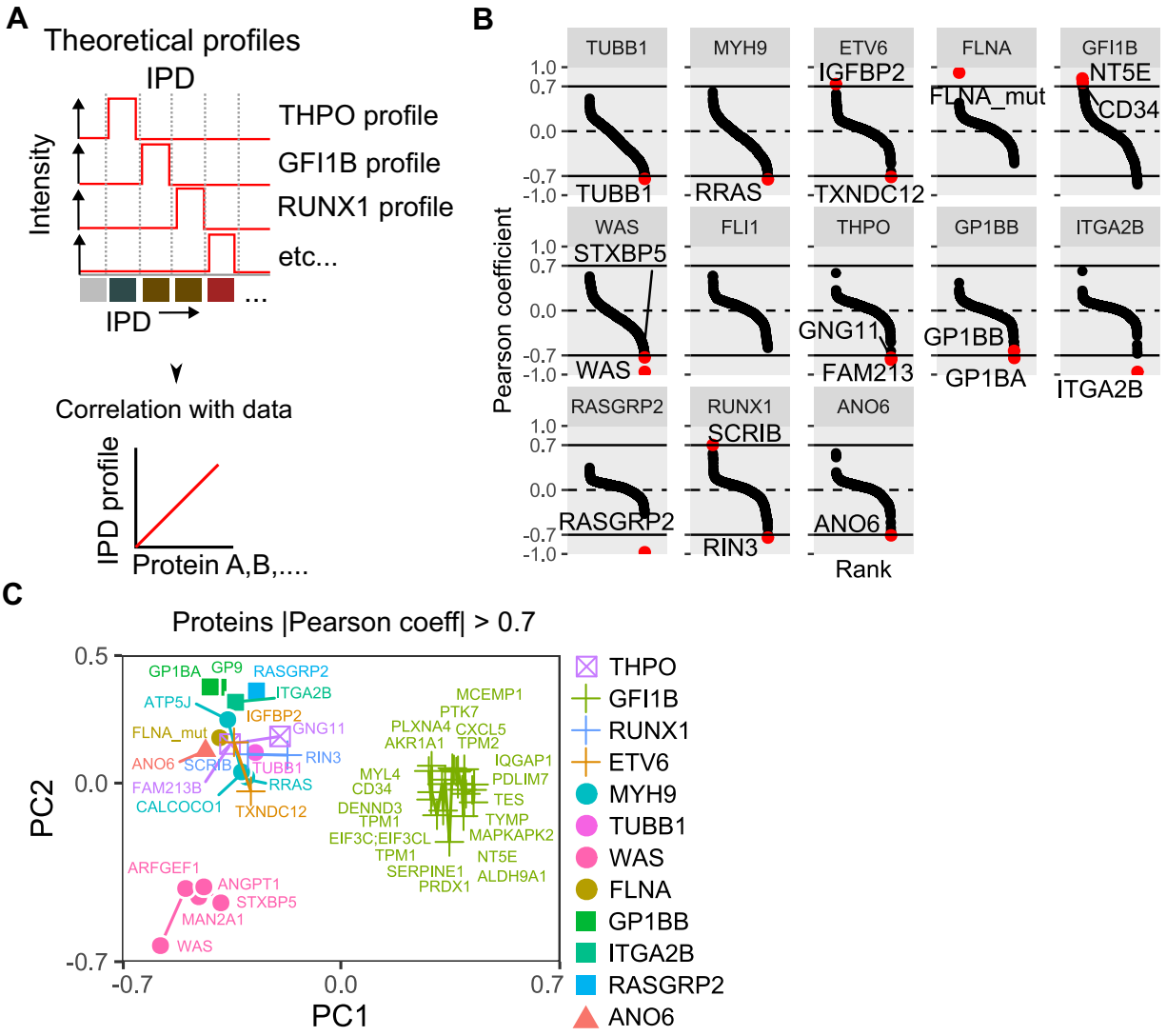

SUPPLEMENTARY FIGURE S2 Scheme showing theoretical specific profile approach. To identify proteins of which the intensity values associate with a given IPD we defined theoretical profiles in which intensities are high for a given IPD and low in all other samples (eg, a LFQ value of 30 in GFI1B samples and a LFQ value of 20 in all other samples). (B) Theoretical profiles defined in (A) were correlated with all quantified proteins. (C) PCA of proteins with absolute Pearson correlation coefficient >0.7 for an IPD-specific profile.

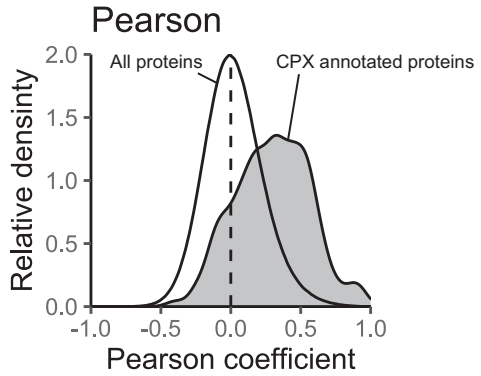

SUPPLEMENTARY FIGURE S3 Density plot of Pearson correlation coefficient for protein-protein correlations. White: distribution of all correlation coefficients. Gray: distribution of correlation coefficients of proteins that are part of protein complexes, annotated using the EMBL-EBI Complex Portal resource.

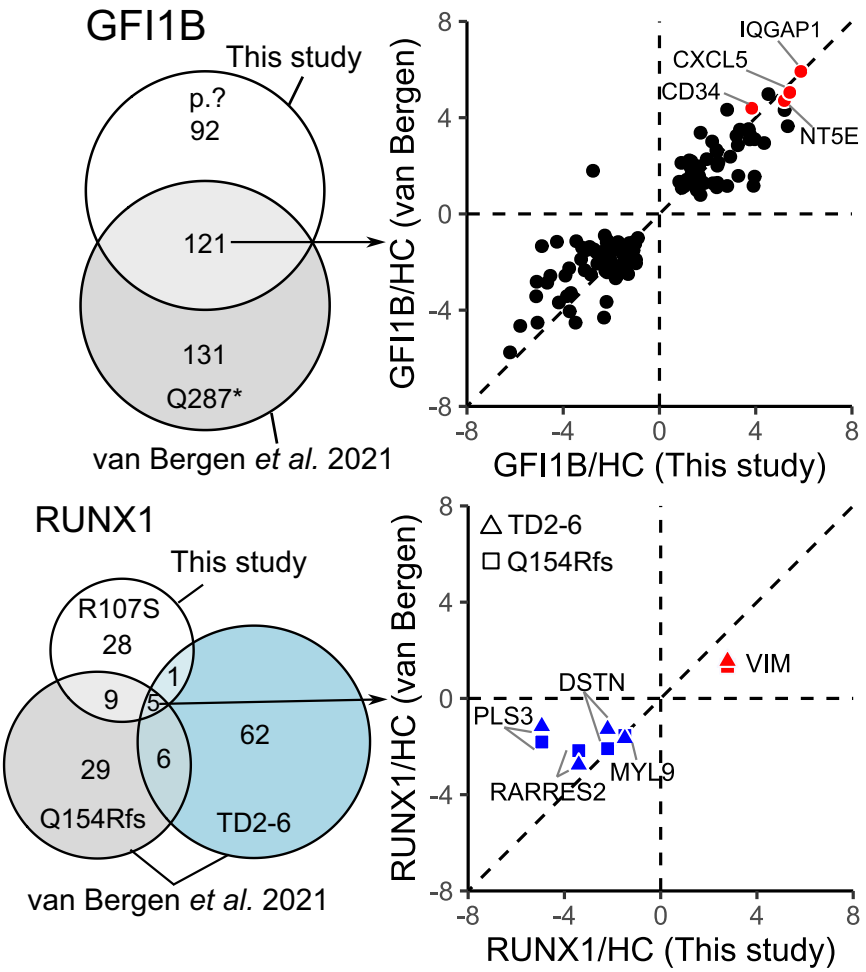

SUPPLEMENTARY FIGURE S4 Comparison of impact of genetic variation in *GFI1B* and *RUNX1* on platelet proteomes in the present study and van Bergen et al. [33]. Venn-diagram shows overlap between differentially abundant proteins. Scatter plots show the median log-fold change of patients vs controls of overlapping proteins.